J. S. Afr. Inst. Min. Metall., vol. 92, no. 10.
Oct. 1992. pp. 275-281.

The effects of flow velocity and pH on the corrosion rate of mild steel in a synthetic minewater

by P.V. Scheers*

SYNOPSIS

A rotating-cylinder electrode (RCE) was used to simulate the effect of flow velocity on pipe corrosion. A comparison is made between the electrochemical measurements obtained and those measured with a laboratory-scale flow loop. There is good general agreement if the speed of rotation of the RCE is adjusted to give the same value of mass-transfer coefficient as in the other system. Hence, it appears that the RCE is well suited to simulate actual flow conditions in pipes.

The simultaneous effect of flow velocity and pH value on the corrosion rate of mild steel in a synthetic minewater was investigated. The increase of corrosion rate was found to be more pronounced at lower pH values and, apart from a sharp increase below pH 4, the initial corrosion rate also increased at pH 7 and 6.

SAMEVATTING

'n Draaisilinderelektrode (DSE) is gebruik om die uitwerking van vloeisnelheid op pypkorrosie te simuleer. Die elektrochemiese metings wat verkry is, is vergelyk met dié wat met 'n laboratoriumskaalvloeilus gemeet is. Daar is 'n goeie algemene ooreenkoms as die rotasiespoed van die DSE aangepas word om dieselfde waarde vir die massaoordragkoëffisiënt as in die ander stelsel te gee. Dit wil dus voorkom of die DSE heeltemal geskik is om werklike vloeitoestande in pype te simuleer.

Die gelyktydige uitwerking van vloeisnelheid en pH-waarde op die korrosietempo van sagte staal in sintetiese mynwater is ondersoek. Daar is gevind dat die toename in die korrosietempo duideliker by die laer pH-waardes is en dat die aanvanklike korrosietempo, afgesien van 'n skerp styging onder 'n pH van 4, ook by 'n pH van 7 en 6 gestyg het.

INTRODUCTION

Failure of equipment due to corrosion is a major problem in the South African mining industry, and pipes, valves, and fittings account for one of the highest expenditures on equipment and spares. Mild steel is still the material most commonly used for pipes in the mining industry. One of the parameters influencing the corrosion of pipe materials is the flow velocity, through its effect on mass transfer and other phenomena such as erosion–corrosion.

One way in which the effects of flow velocity can be studied on a laboratory scale is by the use of a flow loop to simulate real conditions. Unfortunately, such a system is cumbersome to install, and impracticable to operate, especially for the rapid determination of corrosion rates by electrochemical techniques.

In the investigation described here, a rotating-cylinder electrode (RCE) was used to simulate the effect of flow velocity on the corrosion of mild-steel pipes at various pH values, and some of the results were correlated with data obtained with a laboratory flow loop.

THEORETICAL ASPECTS

Flow in pipes is usually turbulent, the transition from laminar to turbulent flow occurring at a critical value of the Reynolds number[1]:

$$Re_{crit} = \frac{U \cdot d}{\upsilon} = 2300. \qquad [1]$$

(All the symbols are defined at the end of this paper.)

Turbulent flow destroys the concentration gradients in the bulk of the fluid, and all the action affecting corrosion then takes place in a very thin boundary layer of fluid adjacent to the pipe wall.

Although the rotating-disk electrode (RDE) is often used to simulate the effects of flow and diffusion, its use is not recommended in this case, since it operates under conditions of laminar flow, even at large values of the Reynolds number. Furthermore, in the case of the rotating disk, the tangential component of velocity at any point depends on the angular velocity and the radius, and a radial component of velocity is also present.

The RCE, however, operates under conditions of turbulent flow. At very low rotational speeds, there is no radial component of the velocity, and the tangential velocity is the same at every point. It is therefore more suitable for the simulation of the effects of flow velocity on the corrosion of pipe materials.

Equations relating mass transport and flow velocity for various geometries have been derived by several authors. As many variables are involved, the most convenient way of handling experimental results is by way of dimensionless groups.

While several equations describing mass transfer in pipes have been deduced theoretically, others have been derived experimentally. These equations are given in terms of the mass-transfer coefficient, the Stanton number, or the Sherwood number but, for convenience, they are all presented in this paper in terms of the Sherwood number.

Colburn's[2] empirical relation can be written

$$Sh = 0{,}0023\, Sc^{1/3} \cdot Re^{0{,}8}, \qquad [2]$$

* Mintek, Private Bag X3015, Randburg, 2125 Transvaal.

 SA ISSN 0038-223X/3.00 + 0.00. Paper received October 1991; revised paper received June 1992.

while Deissler's analysis[3] leads to the relationship

$$Sh = 0{,}022\, Sc^{1/4} \cdot Re^{0{,}875}, \quad [3]$$

and Metzner and Friend's[4] to

$$Sh = 0{,}017\, Sc^{1/3} \cdot Re^{0{,}875}. \quad [4]$$

Harriott and Hamilton[5] measured mass-transfer rates for smooth pipe sections in benzoic acid dissolved in glycerine–water solutions, and their results correlate best with the equation

$$Sh = 0{,}0096\, Sc^{0{,}346} \cdot Re^{0{,}913}. \quad [5]$$

Shaw and Hanratty[6], using an electrochemical technique, found the following relationship:

$$Sh = 0{,}018\, Sc^{0{,}296} \cdot Re^{0{,}875}. \quad [6]$$

Ellison and Schmeal[7] studied the corrosion of carbon-steel pipes in 60 to 96 per cent (by mass) sulphuric acid. They found that their results best fitted the correlation of Harriott and Hamilton (equation [5]).

Mass transfer at the RCE has received considerable attention, and comprehensive reviews have been made by Gabe[8,9]. Although there is some controversy about the characteristic dimension that must be introduced in the Reynolds number for a rotating cylinder, Eisenberg *et al.*[10] showed that the correct dimension was the diameter of the cylinder. The transition from laminar to turbulent flow then occurs at Reynolds numbers between 50 and 200, depending on the surface roughness and other factors[11].

Empirically deduced equations that use dimensionless numbers to relate mass transfer and flow velocity at the RCE have the general form

$$Sh = A \cdot Re^{\cdot a} \cdot Sc^{b}, \quad [7]$$

with values[8] of a ranging from 0,70 to 0,60, and b from 0,41 to 0,339.

Gabe and Robinson[12], using the model of the three-zone electrolyte (concentration-boundary layer, viscous sublayer, and fully developed turbulence), derived the following expression theoretically:

$$Sh = Cte \cdot Re^{2/3} \cdot Sc^{1/3}, \quad [8]$$

and there is hence a good general agreement between the theory and experimental results.

The same authors[13] used a rotating cylinder in tests on the deposition of copper. They found that the rate of mass transfer and prevailing hydrodynamic conditions can be related by

$$Sh = 0{,}169\, Re^{0{,}66} \cdot Sc^{0{,}33}. \quad [9]$$

Other empirical relations were deduced by Arvia *et al.*[14], who found that

$$Sh = 0{,}217\, Re^{3/5} \cdot Sc^{1/3}, \quad [10]$$

and by Cornet and Kappesser[15], who for a Schmidt number of 450 obtained

$$Sh = 0{,}97\, Re^{0{,}639}. \quad [11]$$

The most favoured experimental correlation, however, is that of Eisenberg *et al.*[10]:

$$Sh = 0{,}079\, Re^{0{,}70} \cdot Sc^{0{,}356}. \quad [12]$$

According to equation [12], the mass-transfer coefficient is proportional to the peripheral velocity of the rotating cylinder raised to the 0,7th power—a correlation observed by other authors[16]. In a recent study, Shirkanzadeh[17], using an RCE with heat-transfer facilities, found that, under isothermal conditions, the mass transfer obeys the correlation of Eisenberg *et al.*[10].

The equations mentioned so far are valid for hydrodynamically smooth surfaces, i.e. when the surface irregularities have a height comparable with the thickness of the laminar sublayer. However, the presence of a layer of corrosion products causes some surface roughness, and this results in a friction factor that is independent of the angular velocity for Reynolds numbers greater than a critical Reynolds number, Re_{crit}[18]. The rate is then expected to be a linear function of the Reynolds number. The value of the critical Reynolds number is obtained from the following approximate relation[19,20]:

$$Re_{crit} = (11{,}8\, d/e)^{1{,}18}. \quad [13]$$

Mahato *et al.*[21] made a detailed examination of the effect of surface roughness on the mass-transfer coefficient in the damped turbulence layer and in the corrosion-product layer. They found that the overall mass-transfer coefficient of the corrosion process decreases with an increase in exposure time, and increases with an increase in Reynolds number for small times of exposure. On the other hand, it becomes almost independent of the Reynolds number for long exposure times.

EXPERIMENTAL

The laboratory-scale flow loop consists of a 20-litre tank from which the solution is pumped through several metres of plastic tubing 2,54 cm in diameter. A specially designed electrochemical cell is inserted in the tubing circuit. The working electrode is a ring, with an inside diameter of 2,25 cm and a width of 0,9 cm, that is inserted between two polypropylene sections. A graphite rod, which acts as a counter-electrode, and a Luggin–Haber capillary, which forms the junction with a saturated calomel reference electrode, are also fitted into the cell. A thermostat in the tank maintains the solution at the desired temperature. The

flow velocity measured by means of a flowmeter can be varied from 0 to 220 cm · s^{-1}.

The RCE is driven by a stirrer with a rotational speed that is adjustable between 200 and 5000 r/min. The stainless-steel shaft connected to the stirrer is insulated from the solution by a tightly fitting Teflon sleeve consisting of an upper component 10 cm long and a lower component 3,5 cm long. The electrode, which is 1 cm in length and 2 cm in diameter, is fitted with O-rings between the two Teflon components. Electrical contact to the working electrode is made by means of carbon brushes in contact with a brass sleeve at the top of the stainless-steel shaft.

The electrode is immersed in a glass vessel with three graphite rods (which act as counter-electrodes) and a Luggin–Haber capillary. To control the temperature of the environment, the vessel is immersed in a water-bath that incorporates an automatic temperature controller.

All the experiments were conducted at 45°C in minewater B, which is an artificial 'machine' water[22], i.e. the type of water that is usually found flowing through the general reticulation system of a mine. This artificial water is based on samples of machine water taken from the Orange Free State goldfield, where corrosion problems tend to be greater than those experienced on the Witwatersrand. The composition of minewater B is given in Table I. The pH was adjusted by the addition of dilute H_2SO_4 or NaOH before the start of each test.

Table I

Composition of minewater B, mg · l^{-1}

NaCl	2040
$CaSO_4 \cdot 2H_2O$	1290
$MgSO_4 \cdot 7H_2O$	608
NH_4NO_3	317
KNO_3	216
Na_2SO_4	142
KNO_2	60
$NaHCO_3$	42
$FeSO_4 \cdot 7H_2O$	15
Kaolin	45

A PARC 273 corrosion-measurement system was used in the electrochemical experiments. After the test specimens had been polished on 1200-grit emery paper and degreased with acetone, they were left in the solution at the desired flow velocity for half an hour. A Tafel plot was then recorded from –200 mV to 200 mV versus the corrosion potential at a scanning speed of 0,2 mV · s^{-1}.

The corrosion current was calculated from the polarization resistance value by the Stern–Geary equation[23], and the Tafel slopes were determined by use of PARC M342 corrosion software. Each experiment was conducted in duplicate, and the mean value is quoted here. All the potentials are given with respect to the saturated calomel reference electrode.

RESULTS AND DISCUSSION

Verification of the Hydrodynamics

So that each system (flow loop and RCE) could be checked for its adherence to the hydrodynamic behaviour expected for that geometry, the reduction of oxygen on Monel 400 was examined in 3 per cent sodium chloride[24].

Cathodic polarization curves were recorded at various flow velocities and at two different temperatures. The results confirmed that the oxygen-reduction reaction is controlled by mass transfer at –900 mV. The value of the limiting current was measured at that potential, and the relationships between the measured Sherwood number and the Reynolds number were compared with the relationships given in the literature.

The density and viscosity, as well as the diffusion coefficient for oxygen, were obtained by interpolation from data in the literature[25,26]. The concentration of dissolved oxygen was measured with an oxygen meter. Such a determination of the bulk concentration of oxygen lacks accuracy but, although this can influence the absolute values of the Sherwood number, it does not affect the slope of the predicted relationship between the Sherwood, Schmidt, and Reynolds numbers. The values of these parameters are given in the Addendum.

Figure 1 compares results obtained with the RCE with correlations given in the literature.

It must be noted that the numerical coefficient in the correlation of Eisenberg *et al.*[10], Figure 1(a), was corrected according to the power attributed to the Schmidt number. The experimental results from the RCE closely follow the Robinson and Gabe correlation and, although experimental results over a larger range of Schmidt numbers would be needed to give a full three-dimensional correlation, it can be concluded that the RCE obeys the hydrodynamics expected for that system.

Figure 1(b) compares the results obtained for the flow loop with correlations given in the literature. So that all the relations could be fitted in the same graph, the numerical coefficients were changed according to the power attributed to the Schmidt number. Although there is good general agreement, the experimental points are more scattered than those from the RCE. This could be due to the design of the electrochemical cell inserted in the flow loop.

Observations support the view that the type of core flow is of secondary importance when the mass transfer is controlled by hydrodynamic conditions near the pipe wall[19], and the presence of other surfaces at distances of about 1000 times the thickness of the boundary layer is not expected to influence the rate of mass transfer.

Hence, in the case of the RCE, the counter-electrodes and Luggin capillary have no influence on the hydrodynamic conditions prevailing at the surface of the specimen. However, in the flow-loop electrochemical cell, it is likely that the counter-electrode and Luggin capillary, which are introduced through the wall of the cell near the test sample, to some extent disturb the hydrodynamic conditions at the wall of the sample.

Corrosion Rate and Mass Transfer

So that the degree of control by mass transfer can be estimated, the corrosion rates can be usefully expressed as dimensionless Sherwood numbers:

$$Sh = \frac{i_{corr} \cdot X \cdot d}{(C_b - C_w) \cdot D}, \qquad [14]$$

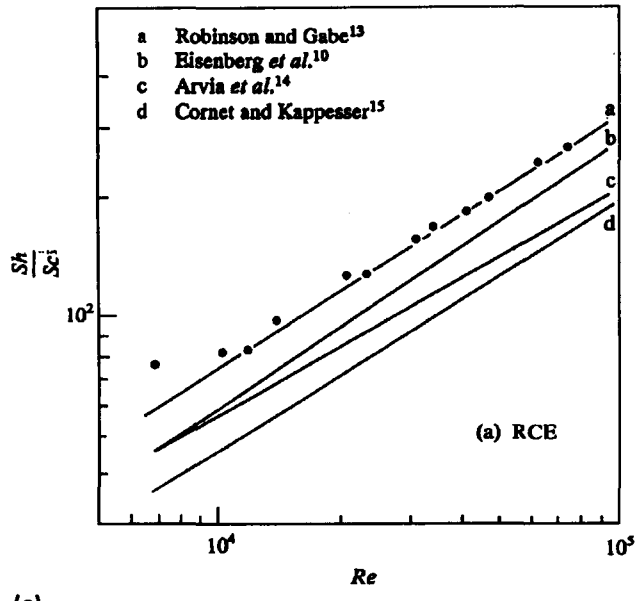

(a)

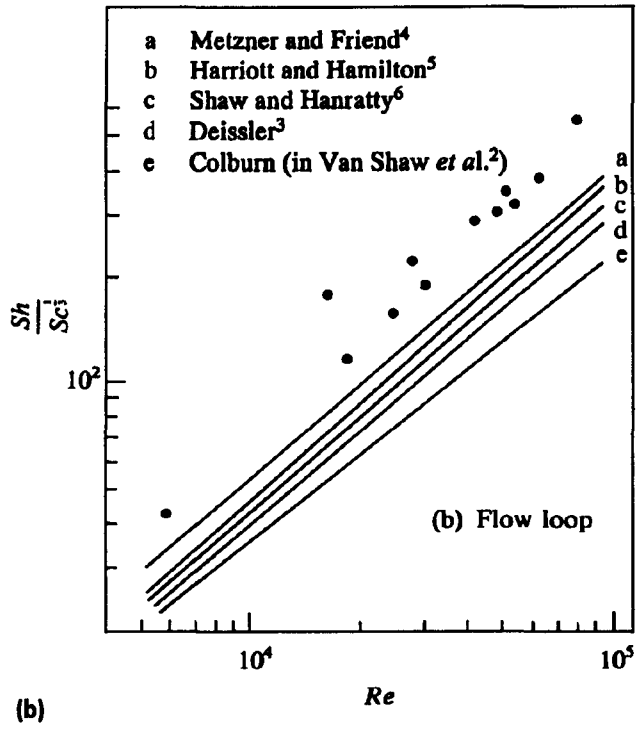

(b)

Figure 1—A comparison of experimental results with mass-transfer correlations from the literature. O_2 reduction on Monel 400 (3% NaCl)

where X is the appropriate factor to convert the corrosion current density into mass flux density. If the corrosion rate is under cathodic control, C_w, the concentration of dissolved oxygen at the wall of the electrode is considered to be zero.

The corrosion rate at pH 7, expressed as the Sherwood number, is compared in Figure 2 with relationships predicted for a process controlled by mass transfer. The areas between the broken lines in Figure 2 represent the flow velocities usually encountered in minewater circuits. (It must be noted that the values of the Reynolds number are given for the RCE and the laboratory-scale flow loop, since an increase in diameter will increase both the Reynolds number and the Sherwood number.) It can be seen that, although the experimental results fall between the predicted relationships, there is some change in the predicted slope for both systems. This could be due to the layer of corrosion products that forms on the electrode. However, the experiments were conducted after the specimen had been immersed for only half an hour, which is too short a time for a decrease in the influence of the Reynolds number to be observed as predicted by Mahato *et al.*[21] for long exposure times; nor is there a linear dependence (slope = 1) between the Sherwood number and the Reynolds number, as was observed by Kappesser *et al.*[20] for rough surfaces. This seems to indicate that, if this deviation in slope is due to the presence of corrosion products, it is not due to their modification of the surface roughness.

Comparison between RCE and Flow Loop

One cannot equate the flow velocity in the flow loop with the peripheral velocity at the RCE since the geometries are different, and the transfer of momentum in each geometry must be taken into consideration.

According to Silverman[27], if the shear stresses in the wall are set equal in the two geometries and similar hydrodynamic conditions, e.g. turbulence, are maintained, the corrosion mechanism (not rate) is hypothesized to be the same in the two geometries.

The shear stress at the wall is given[28] by

$$r = \frac{f}{2} \cdot \rho \cdot U^2 , \qquad [15]$$

where f is the friction factor, which is a function of the Reynolds number. For pipe flow in hydraulically smooth tubes[28],

$$f = 0{,}079\, Re^{-0{,}25} \qquad [16]$$
$$4000 < Re < 10^5$$

while, for a hydraulically smooth cylinder[10],

$$\frac{f}{2} = 0{,}079\, Re^{-0{,}30} . \qquad [17]$$

From a combination of equations [15], [16], and [17], it is possible to deduce the peripheral speeds of the RCE and the flow velocities in the flow loop at which the same values of shear stress at the wall will be obtained in both geometries. The resulting equation is as follows:

$$U_1 = 0{,}665 \frac{d_1^{0{,}176}}{d_2^{0{,}147}} \cdot (\rho/\mu)^{0{,}029} \cdot U_2^{1{,}029} . \qquad [18]$$

On the other hand, equal shear stresses do not necessarily mean equal rates of mass transfer and, if the corrosion reaction is controlled by mass transfer, the mass-transfer coefficient should be equated in the two geometries.

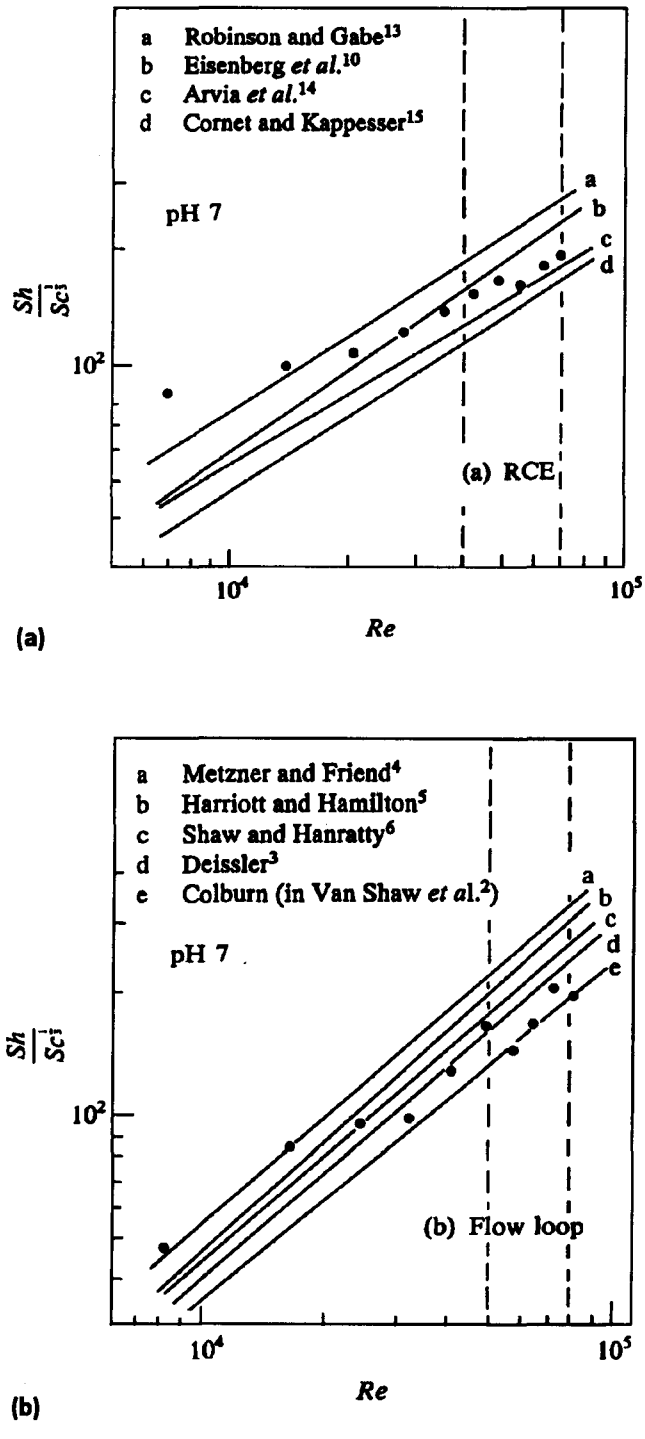

Figure 2—Corrosion rates expressed as Sherwood numbers. (The area between the broken lines represents the usual flow velocity in minewater circuits)

Silverman[27] pointed out that, for the large Schmidt numbers that are normally encountered in liquids, the mass-transfer boundary layer is much smaller than the hydrodynamic boundary layer and, under these circumstances, the scaling velocity should be the friction velocity, and not the bulk velocity. On this basis, he derived the following equation relating the flow velocities for which the mass-transfer coefficients are equal in the two geometries:

$$U_1 = 0,11845(\rho/\mu)^{1/4} \cdot \frac{d_1^{3/7}}{d_2^{5/28}} \cdot Sc^{-0,0857} \qquad [19]$$

The corrosion rates measured at pH 7 with the RCE and in the flow loop are shown in Figures 3(a) and 3(b) as a function of the flow velocity, which has been normalized to yield the same values for shear stress, Figure 3(a), and the same values for mass transfer, Figure 3(b), in the two geometries. It is obvious that, when the mass-transfer coefficients are equated in the two geometries, the influence of the flow velocity on the corrosion rate is very similar for the RCE and the flow loop, although the corrosion rate is somewhat higher when measured at the RCE. The corrosion rates are fairly high, but it must be stressed that they were measured after the specimen had been immersed for only half an hour; the corrosion rate is expected to drop after a longer period.

The same kind of comparison was not possible at more extreme pH values since, at pH 3, the results obtained with the flow loop showed a very large scatter, while, at pH 10, the corrosion rate was too low for a significant comparison of the two geometries.

Influence of Flow Velocity and pH Value

Figure 4 shows the corrosion rate measured at the RCE at three different pH values as a function of the flow velocity. The peripheral speed of the electrode was converted to a pipe-flow velocity that would give the same value for the mass-transfer coefficient. It is worth noting that the flow velocity in minewater circuits is usually around 200 cm · s^{-1}

As shown in Figure 4, the increase in corrosion rate with flow velocity differs according to the pH value. The corrosion rate is lower at pH 10 while, at pH 3, it levels out when the flow velocity reaches a certain value.

The varying influence of flow velocity on corrosion rate is probably correlated with the physical and chemical characteristics of the corrosion-product layer, which differs according to the pH. At pH 10, an adherent protective film would be formed, and this would create an additional barrier to diffusion while, at pH 3, the increased solubility of iron would result in the formation of fewer colloidal particles, which might be deposited on the electrode. Furthermore, at pH 3, disruption of the film by the evolution of hydrogen would tend to expose the metal to the water, resulting in an increase in oxygen depolarization and hydrogen evolution[29]. The corrosion rates measured at pH 3 become independent of flowrate only at high flow velocities, probably when the less adherent and less protective film of corrosion products is physically removed from the surface.

Figure 5 shows the combined effect of pH and flow velocity on the corrosion rate of mild steel in minewater B. It is generally accepted that, between pH 4 and 10, corrosion rate is independent of pH and depends only on how rapidly oxygen diffuses to the metal surface. At pH values of less than 4, the increased corrosion rate is due to both hydrogen evolution and oxygen depolarization.

Figure 5 shows a sharp increase in the corrosion rate below pH 4 but, on the other hand, the corrosion rate also

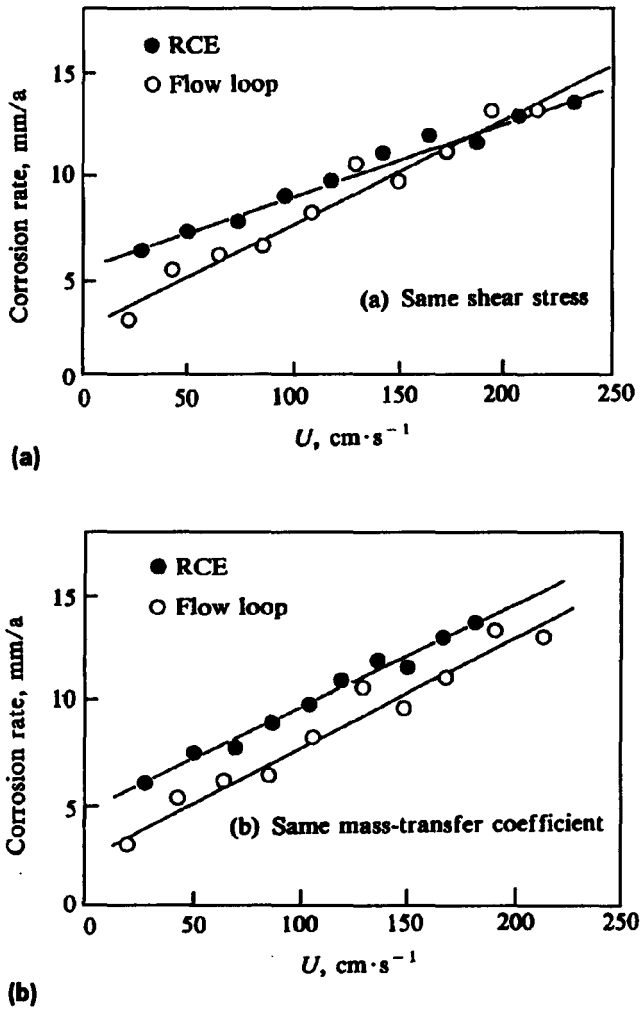

Figure 3—Corrosion rate as a function of the normalized flow velocity (synthetic minewater, pH 7, 45°C)

increases at pH 7 and 6. This phenomenon has also been observed by other authors. Eliassen *et al.*[29] suggested that conflicting results for the effect of pH on corrosion can be explained if the length of the test period is taken into account. In short-term studies (10 days) of the corrosion of steel pipes in synthetic tapwater, they found that, under conditions of flow, the corrosion was less at pH 5 than at pH 7, decreasing again at pH values higher than 7. However, this was not observed at zero velocity, or for longer testing periods (30 to 40 days). They point out that the variations could be caused by changes in the mode of corrosion, and by the nature of the corrosion products formed as a function of time and pH.

Fontana[30] also ascribes such variations at constant velocity to the nature and composition of the surface scale formed. For distilled water at 50°C and high velocity (around 1200 cm · s^{-1}), little attack was observed at pH 6 and 10, but high rates of attack were observed at pH values of 8 and less than 6. The scale on the specimens exhibiting high rates of deterioration was granular in nature and consisted of magnetic Fe_3O_4. Below pH 5, the scale cracked, and fresh metal was exposed. In the regions of low attack, the corrosion products were $Fe(OH)_2$ and $Fe(OH)_3$, which are more protective—probably because they hinder the transfer of oxygen and ions.

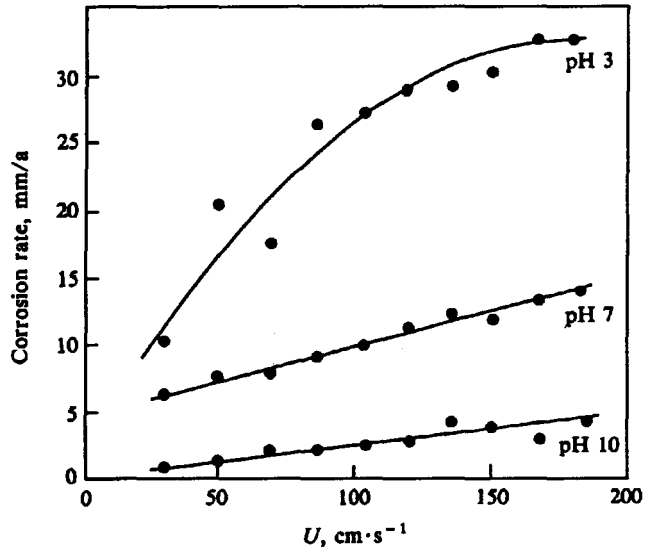

Figure 4—Influence of flow velocity on corrosion rate at different pH values (measured with the RCE)

A more detailed study involving surface analysis would be needed to show the exact part played by the layer of corrosion products.

Mintek has installed water-quality and corrosion-monitoring stations at several mines, but a comparison of the results obtained there with the results of the present work is difficult since, in the field, several parameters have a simultaneous influence on the corrosion rate, and it is difficult to distinguish between their individual contributions. However, it was observed that the corrosion rates measured in the field are always at least one order of magnitude lower than the values mentioned in the present paper. This is hardly surprising since the corrosion rate of mild steel in that kind of environment is known to be fairly high initially, but to decrease to a constant value after about 100 hours[22]. This is due to the formation of corrosion products that slow down the corrosion reaction.

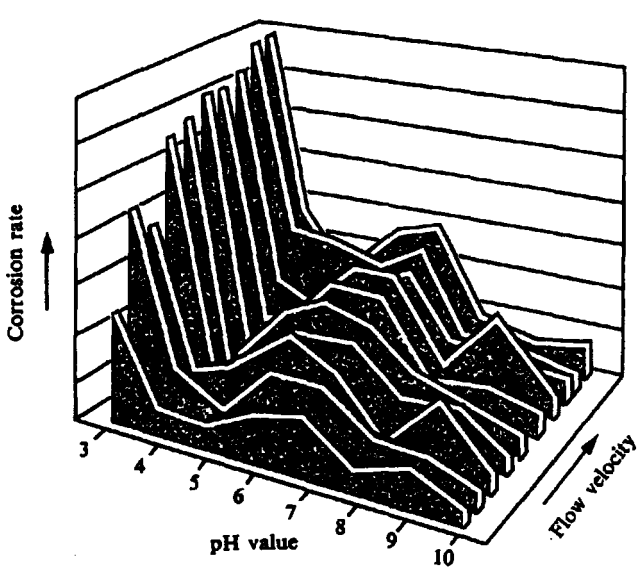

Figure 5—Combined effect of pH value and flow velocity on the corrosion rate of mild steel in minewater B (measured with the RCE)

Hence, although the present work has shown that the RCE is well suited to simulate flow in pipes, longer-term experiments would be necessary to correlate the results with actual conditions.

CONCLUSIONS

The RCE is well suited to the simulation of flow velocity in pipes. The technique appears very useful in showing the effects of flow velocity on the initial corrosion rate of pipe materials, which can easily be determined by electrochemical techniques. The results are usually less scattered and more reproducible than those obtained from an electrochemical cell in a laboratory-scale flow loop.

The observed effects of pH and flow velocity on the corrosion rate of mild steel in minewater B should be correlated with the nature of the corrosion-product layer formed under various conditions of flow velocity and pH.

ACKNOWLEDGEMENT

This paper is published by permission of Mintek.

LIST OF SYMBOLS

A, B Constants
C_b Bulk concentration (mol · cm^{-3})
C_w Concentration at the wall (mol · cm^{-3})
d_1 Diameter of rotating cylinder (cm)
d_2 Diameter of pipe in flow loop (cm)
D Diffusion coefficient (cm^2 · s^{-1})
f Friction factor (dimensionless)
i_{corr} Corrosion current density (A · cm^{-2})
J Mass flux density (mol · cm^{-2} · s^{-1})
k Mass-transfer coefficient ($J/(C_b - C_w)$)
Re Reynolds number ($U \cdot d/\upsilon$)
Sc Schmidt number (υ/D)
Sh Sherwood number ($k \cdot d/D$)
U_1 Peripheral velocity of the rotating cylinder (cm · s^{-1})
U_2 Flow velocity in the flow loop (cm · s^{-1})
μ Absolute viscosity (g·cm^{-1} · s^{-1})
υ Kinematic viscosity (cm^2 · s^{-1})
ρ Density (g · cm^{-3})
τ Wall shear stress (g · cm^{-1} · s^{-2})

REFERENCES

1. SCHLICHTING, H. *Boundary layer theory.* 7th ed. New York, McGraw Hill, 1979. p. 39.
2. Cited in : VAN SHAW, P., REISS, L.P., and HANRATTY, T.J. *AIChE J.*, vol. 9. 1963. pp. 362-364.
3. DEISSLER, R.G. *Natl. Advisory Comm. Aeronaut., Tech. Note* 1210, 1955.
4. METZNER, A.B., and FRIEND, W.L. *Can. J. Chem. Eng.*, vol. 26, 1958. p. 255.
5. HARRIOTT, P., and HAMILTON, P.M. *Chem. Eng. Sci.*, vol. 20. 1965. pp. 1073-1078.
6. SHAW, D.A., and HANRATTY, T.J. *AIChE J.*, vol. 23. 1977. pp. 28-37.
7. ELLISON, B.T., and SCHMEAL, W.R. *J. Electrochem. Soc.*, vol. 125. 1978. pp. 524-531.
8. GABE, D.R. *J. Appl. Electrochem.*, vol. 4. 1974. pp. 91-108.
9. GABE, D R., and WALSH, F.G. *J. Appl. Electrochem.*, vol. 13. 1983. pp. 3-22.
10. EISENBERG, M., TOBIAS, C.W., and WILKE, C.R. *J. Electrochem. Soc.*, vol. 101. 1954. pp. 306-319.
11. GABE, D.R., and ROBINSON, D.J. *Electrochim. Acta*, vol. 17. 1972. pp. 1121-1127.
12. GABE, D.R., and ROBINSON, D.J. *Electrochim. Acta*, vol. 17. 1972. pp. 1129-1137.
13. ROBINSON, D.J., and GABE, D.R., *Trans. Inst. Metal Finish.*, vol. 48. 1970. pp. 35-42.
14. ARVIA, A.J., CAROZZA, J.S.W., and MARCHIANO, S.L. *Electrochim. Acta*, vol. 9. 1964. pp. 1483-1495.
15. CORNET, I., and KAPPESSER, R. *Trans. Inst. Chem. Eng.*, vol. 47. 1969. pp. T194-T197.
16. ARVIA, A.J., and CARROZZA, J.S.W. *Electrochim. Acta*, vol. 7. 1962. pp. 65-78.
17. SHIRKANZADEH, M. *Corrosion*, vol. 43. 1987. pp. 621-623.
18. THEODORSEN, T., and REGIER, A. *NACA Ann. Reports*, vol. 793. 1945. p. 156.
19. MAKRIDES, A.C., and HACKERMAN, N. *J. Electrochem. Soc.*, vol. 105. 1958. pp. 156-162.
20. KAPPESSER, R., CORNET, I., and GREIF, R. *J. Electrochem. Soc.*, vol. 118. 1971. pp. 1957-1959.
21. MAHATO, B.K., CHA, C.Y., and SHEMILT, L.W. *Corros. Sci.*, vol. 20. 1980. pp. 421-441.
22. HIGGINSON, A. The effect of physical and chemical factors on the corrosivity of a synthetic mine water. Randburg, Mintek, *Report* M140.
23. STERN, M., and GEARY, A.L. *J. Electrochem. Soc.*, vol. 104. 1957. pp. 56-63
24. SILVERMAN, D.C. *Corrosion*, vol. 40, 1984. pp. 220-226.
25. *International critical tables.* New York, McGraw Hill, 1933.
26. *Handbook of tables for applied engineering science.* Cleveland, (USA), The Chemical Rubber Company, 1970.
27. SILVERMAN, D.C. *Corrosion*, vol. 44. 1988. pp. 42-49.
28. BEEK, W.J., and MUTTZALL, K.M.K. *Transport phenomena.* London, John Wiley, 1975. p. 55.
29. ELIASSEN, R., PERRDA, C., ROMBO, A.J., and SKRINDE, R.T. *AWWA*, vol. 48. 1956. pp. 1005-1018.
30. FONTANA, M.G. *Corrosion engineering.* 3rd ed. New York, McGraw Hill, 1987. p. 94.

ADDENDUM: VALUES OF PHYSICAL PARAMETERS

(a) *3% NaCl*

Viscosity (g · cm^{-1} · s^{-1}):	25°C	0,94 · 10^{-2}
	45°C	0,63 · 10^{-2}
Density (g · cm^{-3}):	25°C	1,018
	45°C	1,011
O_2 bulk concentration (mol · cm^{-3}):	25°C	2,0 · 10^{-7}
	45°C	1,5 · 10^{-7}
O_2 diffusion coefficient (cm^2 · s^{-1}):	25°C	2,06 · 10^{-5}
	45°C	3,28 · 10^{-5}

(b) *Synthetic mine water (45 °C)*

Viscosity (g · cm^{-1} · s^{-1}) : 0,59 · 10^{-2}

Density (g · cm^{-3}) : 0,99

O_2 bulk concentration (mol · cm^{-3}): 1,7 · 10^{-7}

O_2 diffusion coefficient (cm^2 · s^{-1}): 3,28 · 10^{-5}